

$B_{30}H_8$, $B_{39}H_9^{2-}$, $B_{42}H_{10}$, $B_{48}H_{10}$, and $B_{72}H_{12}$: polycyclic aromatic snub hydroboron clusters analogous to polycyclic aromatic hydrocarbons

Hui Bai · Qiang Chen · Ya-Fan Zhao · Yan-Bo Wu ·
Hai-Gang Lu · Jun Li · Si-Dian Li

Received: 18 July 2012 / Accepted: 7 October 2012 / Published online: 16 November 2012
© Springer-Verlag Berlin Heidelberg 2012

Abstract Calculations performed at the ab initio level using the recently reported planar concentric π -aromatic $B_{18}H_6^{2+}$ (**1**) [Chen Q et al. (2011) *Phys Chem Chem Phys* 13:20620] as a building block suggest the possible existence of a new class of $B_{3n}H_m$ polycyclic aromatic hydroboron (PAHB) clusters— $B_{30}H_8$ (**2**), $B_{39}H_9^{2-}$ (**3**), $B_{42}H_{10}$ (**4/5**), $B_{48}H_{10}$ (**6**), and $B_{72}H_{12}$ (**7**)—which appear to be the inorganic analogs of the corresponding C_nH_m polycyclic aromatic hydrocarbon (PAHC) molecules naphthalene $C_{10}H_8$, phenalenyl anion $C_{13}H_9^-$, phenanthrene/anthracene $C_{14}H_{10}$, pyrene $C_{16}H_{10}$, and coronene $C_{24}H_{12}$, respectively, in a universal atomic ratio of B:C=3:1. Detailed canonical molecular orbital (CMO), adaptive natural density partitioning (AdNDP), and electron localization function (ELF) analyses indicate that, as they are hydrogenated fragments of a boron snub sheet [Zope RR, Baruah T (2010) *Chem Phys Lett* 501:193], these PAHB clusters are aromatic in nature, and exhibit the formation of islands of both σ - and π -aromaticity. The predicted ionization potentials of PAHB neutrals and electron detachment energies of small PAHB monoanions should permit them to be

characterized experimentally in the future. The results obtained in this work expand the domain of planar boron-based clusters to a region well beyond B_{20} , and experimental syntheses of these snub $B_{3n}H_m$ clusters through partial hydrogenation of the corresponding bare B_{3n} may open up a new area of boron chemistry parallel to that of PAHCs in carbon chemistry.

Keywords Polycyclic aromatic hydroboron clusters · Ab initio calculations · Geometrical structures · Electronic structures · Aromaticity

Introduction

Boron, the prototype of electron-deficient elements in the periodic table, has multicenter two-electron (mc-2e) bonds and a rich chemistry, second only to carbon. Boron hydrides B_nH_m ($n=2-20$, $n < m$) play an essential role in advancing the chemistry of boron and, more generally, the theory of how elements bond to each other [1, 2]. Small boron hydride clusters reported in the literature include B_2H_4 [3], BH_3 , B_2H_6 , B_3H_7 , B_4H_{10} , B_5H_9 , and B_5H_{11} [4], B_nH^+ ($n=1-13$) [5], B_2H^+ , $B_2H_2^+$, and $B_3H_2^+$ [6], $B_2H_{2n}^{2+}$ dications ($n=1-4$) [7], B_nH_n neutrals ($n=5-13$, 16, 19, 22), and, more typically, their cage-like dianions $B_nH_n^{2-}$ ($n=5-13$) [1, 2, 8–10]. A unifying “mno” rule has been proposed for polycondensed boranes [11, 12]. Detailed theoretical investigations on a series of small, hydrogen-rich boron hydride clusters with less than five boron atoms have also been reported recently [13–16]. However, little is known about the nature of the partially hydrogenated boron-rich B_nH_m clusters that possess fewer hydrogen atoms than boron ($n > m$). Examples of these clusters include the planar or quasi-planar $B_7H_2^-$ [17, 18], B_4H_n ($n=1-3$) [19], $B_6H_5^+$ [20], $B_{12}H_n$ ($n=$

Electronic supplementary material The online version of this article (doi:10.1007/s00894-012-1640-8) contains supplementary material, which is available to authorized users.

H. Bai · Q. Chen · Y.-B. Wu · H.-G. Lu · S.-D. Li (✉)
Institute of Molecular Sciences, Shanxi University,
Taiyuan 030001, Shanxi, People's Republic of China
e-mail: lisidian@sxu.edu.cn

S.-D. Li
e-mail: lisidian@yahoo.com

Y.-F. Zhao · J. Li
Department of Chemistry, Tsinghua University,
Beijing 100084, People's Republic of China

Q. Chen · S.-D. Li
Institute of Materials Science, Xinzhou Teachers' University,
Xinzhou 034000, Shanxi, People's Republic of China

1–6) [21, 22], $B_{16}H_6$ [23], $B_{18}H_n$ ($n=1-6$) [24], $B_6H_3^+$, and B_8H_4 [25]. Our group recently performed a systematic first-principles investigation of double-chain planar B_nH_2 neutrals ($n=4, 6, 8, 10, 12$) and $B_nH_2^-$ monoanions ($n=3, 5, 7, 9, 11$), which were found to be the boron hydride analogs of conjugated hydrocarbons, suggesting that boron double chains (DCs) in boron hydride clusters correspond to carbon single chains (SCs) in conjugated hydrocarbons [26]. This prediction was confirmed very recently in a combined photoelectron spectroscopy (PES) and ab initio investigation [27]. The evidence accumulated so far strongly suggests that partial hydrogenation leads to planarization in small, boron-rich B_nH_m clusters, and there is an interesting analogous relationship between planar hydroboron clusters and their hydrocarbon counterparts in dual spaces that needs to be fully explored.

Small, pure B_n^- boron clusters up to $n=21$ have been confirmed to possess planar or quasi-planar geometries in triangular motifs according to PES measurements combined with ab initio investigations [2, 13–17, 28–34], while at the infinite 2D limit, both the boron α -sheet (which is theoretically predicted to be the most stable structure [35–37]) and the boron snub sheet (which is the second most stable and is only 0.02 eV/atom less stable than the former [38]) are composed of hybrids of triangular and hexagonal motifs with evenly distributed hexagonal holes surrounded by extended or zigzag DCs (a boron snub sheet can be constructed from a hexagonal sheet using the snub operation [38]). The discovery that hexagonal holes act as electron acceptors and interwoven DCs act as electron donors in stable boron sheets is important [37]. Various lines of evidence indicate that it is necessary to include a suitable proportion of hexagonal holes in 2D boron sheets to avoid buckling. Interestingly, partial hydrogenation at the corner positions of B_n clusters ($n \geq 18$) along their peripheries also leads to the formation of hexagonal hole(s) at the centers of the B_nH_m clusters, as we demonstrated for the recently reported planar concentric π -aromatic species $D_{3h} B_{18}H_3^-$, $D_{2h} B_{18}H_4$, $C_{2v} B_{18}H_5^+$, and $D_{6h} B_{18}H_6^{2+}$, which are the smallest species that consist of a hybrid of triangular and hexagonal motifs with a hexagonal hole at the center [24]. This phenomenon originates from the fact that partial hydrogenation of B_n clusters at the corner positions elongates the peripheral B–B bond lengths and helps to create cavities in 2D boron sheets that can host hexagonal holes. A close comparison between the boron snub sheet [38] with the popular graphene structure [39] indicates that the zigzag boron DCs in the former function in a similar way to the zigzag carbon SCs in the latter. It is well known in organic chemistry that polycyclic aromatic hydrocarbon (PAHC) molecules like benzene C_6H_6 , naphthalene $C_{10}H_8$, anthracene $C_{14}H_{10}$, and coronene $C_{24}H_{12}$ can be viewed as terminally hydrogenated fragments of graphene at corner positions. This inspired us to attempt to design polycyclic aromatic hydroboron (PAHB) clusters by partially hydrogenating fragments of boron snub

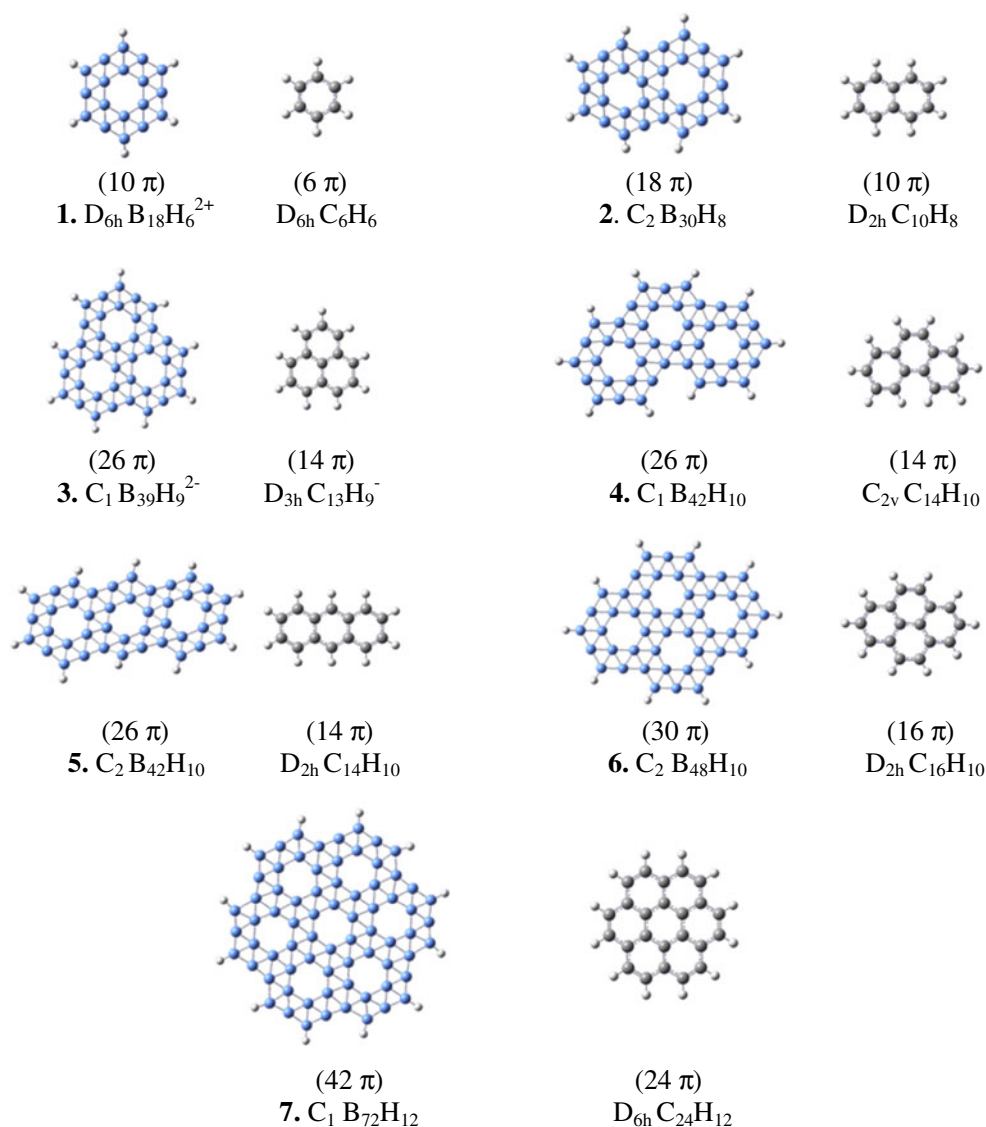
sheet at corner positions, yielding inorganic analogs of the corresponding PAHC molecules. That work is described in the present paper.

Based on the analyses presented above, and starting from the monocyclic species $B_{18}H_6^{2+}$ (1) that we reported previously [24], we therefore explored the possibility, via calculations performed at the ab initio level, of a new class of PAHB clusters $B_{3n}H_m$, including $B_{30}H_8$ (2), $B_{39}H_9^{2-}$ (3), $B_{42}H_{10}$ (4/5), $B_{48}H_{10}$ (6), and $B_{72}H_{12}$ (7), which are created by terminally hydrogenating fragments of the snub sheet at each corner position. These species were found to be inorganic analogs of the corresponding PAHC C_nH_m molecules naphthalene $C_{10}H_8$, phenalenyl anion $C_{13}H_9^-$, anthracene/phenanthrene $C_{14}H_{10}$, pyrene $C_{16}H_{10}$, and coronene $C_{24}H_{12}$, respectively, according to the atomic ratio B:C=3:1. Detailed canonical molecular orbital (CMO), adaptive natural density partitioning (AdNDP) [40–43], and electron localization function (ELF) [44–46] analyses indicated that these polycyclic hydroboron clusters are aromatic in nature, exhibiting both island σ - and π -aromaticity. These snub $B_{3n}H_m$ clusters expand the domain of planar boron-based clusters to a region well beyond B_{20} and experimental syntheses, and characterizations of these planar boron hydride species may establish a clear analogous relationship between planar hydroboron clusters and their hydrocarbon counterparts.

Theoretical procedures

Starting from the previously reported concentric planar species $B_{18}H_6^{2+}$ [24], initial PAHBs were constructed by successively adding edge-sharing B_{18} substructures with two neighboring B_{18} units sharing a B_6 DC rhombus (see Fig. 1 and Scheme 2). These designed PAHBs, which correspond to fragments of the snub sheet that are terminally hydrogenated at each corner position, were then fully optimized using both the hybrid density functional theoretical (DFT) method called B3LYP [47, 48] and the second-order Møller–Plesset approach (MP2) [49–53] with the 6-311+G(d,p) basis set implemented in Gaussian 03 [54]. The two approaches produced essentially the same optimized structures (with slightly different orders of molecular orbital energies in some cases). The optimized planar or quasi-planar PAHBs without imaginary vibrational frequencies are compared with their counterpart PAHCs in Fig. 1. More extensive structure searches were performed for $B_{18}H_6^{2+}$, $B_{30}H_8^{2+}$, and $B_{30}H_8$ using a basin-hopping procedure [55] compiled by Yan-Fan Zhao (alternative low-lying isomers of $B_{30}H_8^{2+}$ and $B_{30}H_8$ are summarized in Figs. S1 and S2 of the “Electronic supplementary material,” ESM). The CMOs and AdNDP [40, 41] bonding patterns of the quasi-planar dicyclic species $C_2 B_{30}H_8$ are compared with those of $D_{2h} C_{18}H_{16}$ and $D_{2h} C_{10}H_8$ in Figs. 2 and 3, respectively (the B3LYP functional has proven to be advantageous

Fig. 1 Optimized structures of the snub PAHB clusters $B_{3n}H_m$ ($n=6, 10, 13, 14, 16,$ and 24 ; $m=6, 8, 9, 10, 10,$ and 12) compared with those of the corresponding PAHC molecules C_nH_m , with the numbers of delocalized π -electrons indicated in parentheses



for ADNDP analyses of various inorganic and organic compounds, including boron clusters and boron hydride clusters [22–29, 40, 41]). Table 1 tabulates the ELF [44–46] bonding patterns and the corresponding bifurcation values of the perfectly planar $D_{6h} B_{18}H_6^{2+}$, $C_{2h} B_{30}H_8$, $C_{3h} B_{39}H_9^{2-}$, $C_s B_{42}H_{10}$, $C_{2h} B_{42}H_{10}$, $C_{2h} B_{48}H_{10}$, and $C_{6h} B_{72}H_{12}$ species, with Fig. 4 showing the ELFs of the infinite 2D snub sheet. The simulated PES spectra of $C_2 B_{30}H_8^-$, $C_1 B_{39}H_9^-$, $C_2 B_{42}H_{10}^-$, and $C_1 B_{42}H_{10}^-$ monoanions are depicted in Fig. 5.

Results and discussions

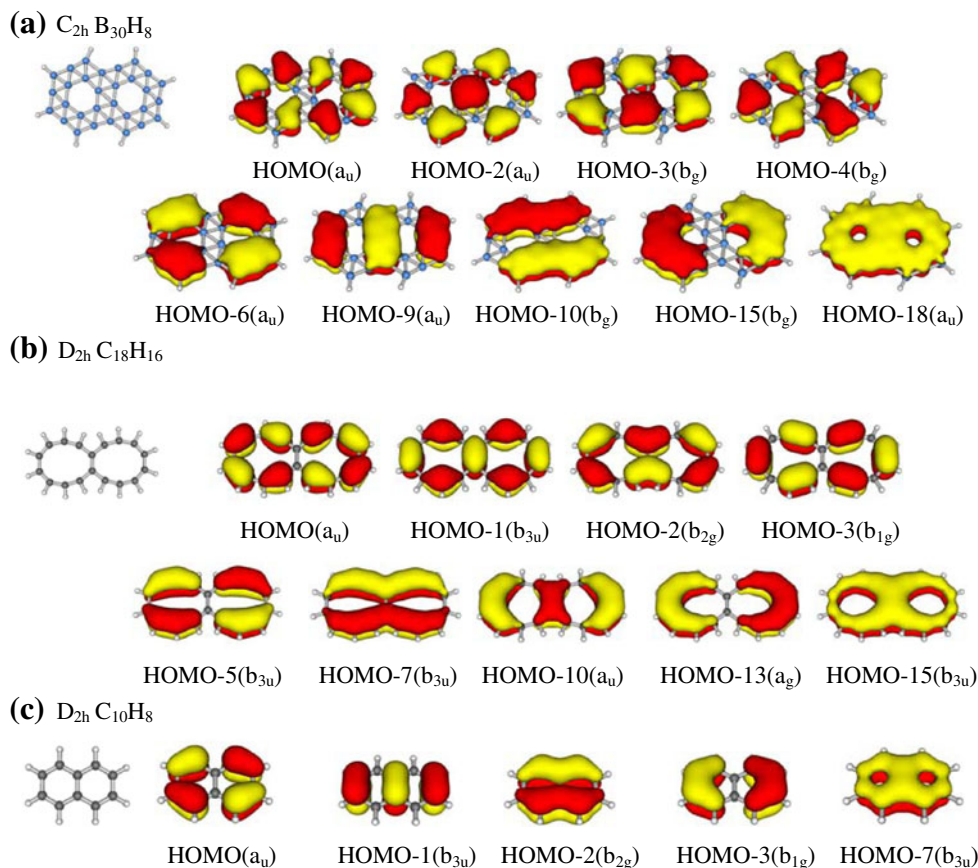
Structures and stabilities

We checked the thermodynamic and dynamic stabilities of the monocyclic species $D_{6h} B_{18}H_6^{2+}$ (**1**) [24], which is the boron hydride analog of benzene, first. Extensive basin-

hopping minimum searches [55] again indicate that this perfectly planar concentric π -aromatic structure with an average B–B bond length of $r_{B-B} \approx 1.66$ Å is truly a deep minimum of the system, lying at least 51 kcal/mol lower than all the other low-lying 2D and 3D isomers obtained [24]. Molecular dynamic (MD) simulations further show that the hexagonal framework and basic atomic connections of the $B_{18}H_6^{2+}$ (**1**) structure remain intact during MD simulations (Merino G, 2012, private communication). Thus, the concentric aromatic planar species $B_{18}H_6^{2+}$ (**1**) is both thermodynamically and dynamically stable. This beautiful hexagonal dication with ten delocalized π -electrons serves as the building block for the PAHB clusters (see Fig. 1) and the boron snub sheet explored in this work, just as the well-known molecule benzene, with six delocalized π -electrons, is the building block of PAHC molecules and graphene.

The quasi-planar dicyclic species $C_2 B_{30}H_8$ (**2**), the second member of the PAHB family, which is analogous to

Fig. 2 Delocalized π -CMOs of C_{2h} $B_{30}H_8$ (a) compared with those of D_{2h} $C_{18}H_{16}$ (b) and D_{2h} $C_{10}H_8$ (c)



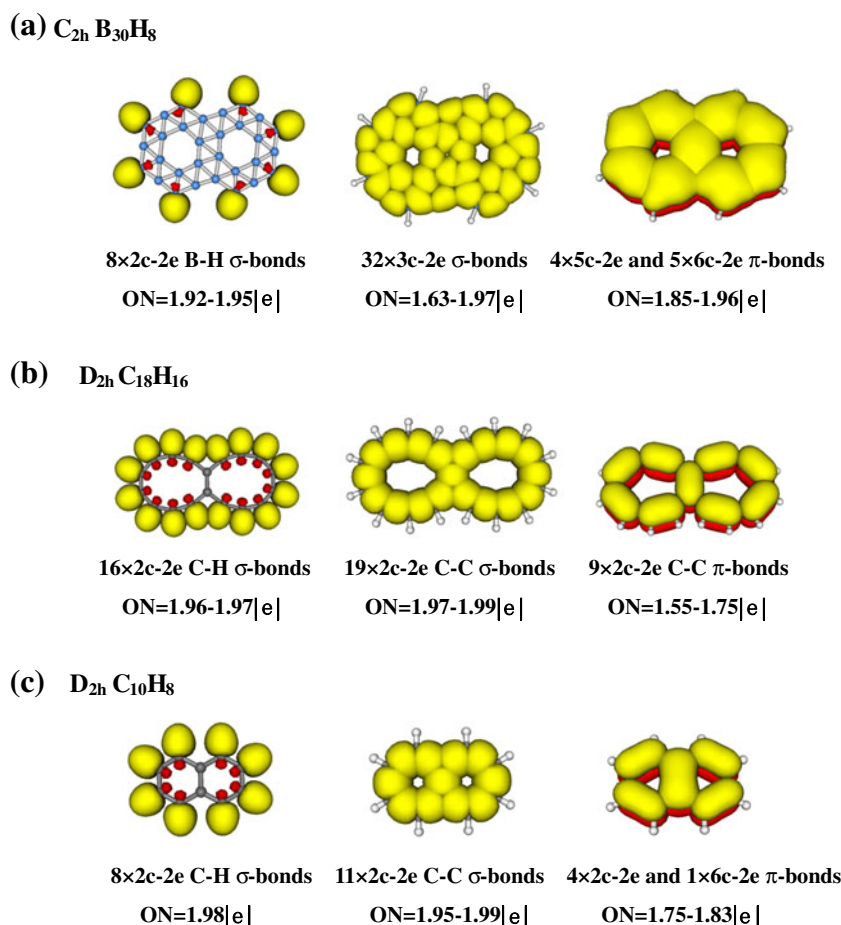
naphthalene D_{2h} $C_{10}H_8$ and has an average B–B bond length of $r_{B-B} \approx 1.67$ Å, appears to lie at least 17 kcal/mol lower than other low-lying 2D and 3D structures obtained (see Fig. S1). It shows slight distortion from the perfectly planar C_{2h} $B_{30}H_8$, which lies 7.8 kcal/mol higher in energy (see Fig. S1 in the ESM and Table 1). Extensive basin hopping minimum searches show that perfect planarity is achieved in its dicyclic dication C_{2h} $B_{30}H_8^{2+}$ ($r_{B-B} \approx 1.67$ Å), which is the vibrationally averaged structure of the system lying at least 49 kcal/mol lower than the other low-lying isomers obtained (the perfectly planar C_{2h} $B_{30}H_8^{2+}$ appears to be 0.006 kcal/mol more stable than the slightly distorted quasi-planar C_2 $B_{30}H_8^{2+}$ with zero-point correction included; see Fig. S2).

For PAHBs with more than two hexagonal holes, the quasi-planar tricyclic C_1 $B_{39}H_9^{2-}$ (3), tricyclic C_1 $B_{42}H_{10}$ (4), tricyclic C_2 $B_{42}H_{10}$ (5), tetracyclic C_2 $B_{48}H_{10}$ (6), and heptacyclic C_1 $B_{72}H_{12}$ (7) species appear to be analogous to phenalenyl anion D_{3h} $C_{13}H_9^-$, phenanthrene C_{2v} $C_{14}H_{10}$, anthracene D_{2h} $C_{14}H_{10}$, pyrene D_{2h} $C_{16}H_{10}$, and coronene D_{6h} $C_{24}H_{12}$, respectively, based on a universal atomic ratio of B:C=3:1. The linear anthracene-like C_2 $B_{42}H_{10}$ (5) turns out to be only 1.0 kcal/mol more stable than the saddle-shaped phenanthrene-like C_1 $B_{42}H_{10}$ (4). These polycyclic PAHBs with average B–B bond lengths of $r_{B-B} = 1.66 \sim 1.68$ Å are all found to be more stable than

their typical double-ring and triple-ring tubular isomers (see examples in Fig. S3). The high stability of the zigzag DCs in these PAHBs agrees with the observation that extended boron DCs are present in the conjugated DC planar C_{2h} B_4H_2 , C_{2h} B_8H_2 , and C_{2h} $B_{12}H_2$ species [26, 27]. We conclude that the formation of the zigzag boron DCs around the evenly distributed hexagonal holes helps to maintain the stability of these planar PAHBs and the boron snub sheet.

To further investigate the thermodynamic stabilities of the PAHB clusters concerned in this work, we calculated the energy differences of the most stable double-ring tubular B_{30} and triple-ring B_{42} and B_{48} [56] from their corresponding partially hydrogenated PAHB clusters. As shown in Scheme 1, the distorted double-ring tubular species C_2 $B_{30}H_8$ (1A) formed by the hydrogenation of the double-ring tubular species C_i B_{30} possesses a hydrogenation energy of 44.61 kcal/mol with respect to $B_{30}(C_i) + 4H_2 = B_{30}H_8(C_2)$. However, this double-ring tubular isomer lies much higher (102.66 kcal/mol) in energy than the quasi-planar dicyclic species C_2 $B_{30}H_8$ (1), which has a hydrogenation energy of 147.27 kcal/mol with respect to $B_{30}(C_i) + 4H_2 = B_{30}H_8(C_2, 1)$. Similarly, tricyclic C_2 $B_{42}H_{10}$ (5) and tetracyclic C_2 $B_{48}H_{10}$ (6) (which are more stable than their triple-ring tubular isomers C_s $B_{42}H_{10}$ and C_s $B_{48}H_{10}$, as indicated in Scheme 1), possess hydrogenation energies of 160.77 and 229.18 kcal/mol with respect to the triple-ring

Fig. 3 σ - and π -AdNDP bonding patterns of planar C_{2h} $B_{30}H_8$ (a) compared with those of D_{2h} $C_{18}H_{16}$ (b) and D_{2h} $C_{10}H_8$ (c), with the occupation numbers (ON) indicated



tubular C_i B_{42} and C_8 B_{48} species, respectively. Given their huge hydrogenation energies with respect to the most stable multi-ring tubular B_n , PAHB clusters are expected to be thermodynamically stable in the gas phase.

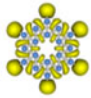
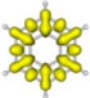
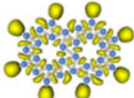
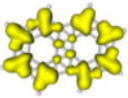
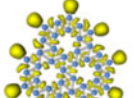

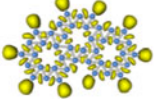
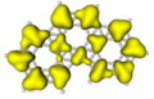
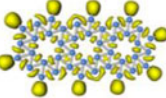
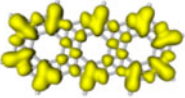
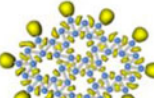
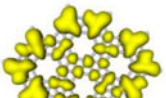
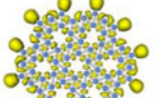
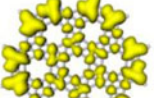
CMO and AdNDP analyses

Canonical molecular orbitals provide vital information on the chemical bonding of PAHBs. For simplicity and clarity, Fig. 2a shows the nine delocalized π -CMOs of the perfectly planar C_{2h} $B_{30}H_8$ [which has very similar π -CMOs to the slightly distorted C_2 $B_{30}H_8$ (2)], including HOMO(a_u), HOMO-2(a_u), HOMO-3(b_g), HOMO-4(b_g), HOMO-6(a_u), HOMO-9(a_u), HOMO-10(b_g), HOMO-15(b_g), and HOMO-18(a_u), which have a clear one-to-one correspondence with the CMOs of D_{2h} $C_{18}H_{16}$ [HOMO(a_u), HOMO-1(b_{3u}), HOMO-2(b_{2g}), HOMO-3(b_{1g}), HOMO-5(b_{3u}), HOMO-10(a_u), HOMO-7(b_{3u}), HOMO-13(a_g), and HOMO-15(b_{3u})] (though there is an exchange of correspondence between HOMO-7(b_{3u}) and HOMO-10(a_u) for D_{2h} $C_{18}H_{16}$ with respect to the MO energy levels) (see Fig. 2b). It should be mentioned that the dicyclic species D_{2h} $C_{18}H_{16}$ is not even a local minimum of the system, similar to the situation observed in monocyclic D_{10h} $C_{10}H_{10}$ [24, 29]. Also note that

the five low-lying MOs of C_{2h} $B_{30}H_8$ [HOMO-6(a_u), HOMO-9(a_u), HOMO-10(b_g), HOMO-15(b_g), and HOMO-18(a_u)] correspond exactly to the five delocalized π -CMOs of naphthalene D_{2h} $C_{10}H_8$ [HOMO(a_u), HOMO-1(b_{3u}), HOMO-2(b_{2g}), HOMO-3(b_{1g}), and HOMO-7(b_{3u}), respectively]. Obviously, C_{2h} $B_{30}H_8$ (2) with 18 delocalized π -electrons formally conforms to the $4n+2$ Huckel rule ($n=4$) in the overall π -electron count, similar to both aromatic D_{2h} $C_{18}H_{16}$ with 18 π -electrons ($n=4$) and D_{2h} $C_{10}H_8$ with 10 π -electrons ($n=2$) (see Fig. 2). The C_{2h} $B_{30}H_8^{2+}$ dication is found to have the same π -CMOs as C_{2h} $B_{30}H_8$ at both the MP2 and B3LYP levels of theory. Detailed CMO analyses show that tricyclic C_i $B_{39}H_9^{2-}$ (3), tricyclic C_i $B_{42}H_{10}$ (4), tricyclic C_2 $B_{42}H_{10}$ (5), tetracyclic C_2 $B_{48}H_{10}$ (6), and heptacyclic C_i $B_{72}H_{12}$ (7) possess 26, 26, 26, 30, and 42 delocalized π -electrons, respectively (see Fig. S4), formally conforming to the $4n+2$ rule in their total numbers of π -electrons.

AdNDP analysis has proven to be an effective tool for analyzing the bonding patterns of various organic and inorganic molecules [40–43]. As an example, Fig. 3 compares the AdNDP bonding pattern of C_{2h} $B_{30}H_8$ (a) with that of D_{2h} $C_{18}H_{16}$ (b), and D_{2h} $C_{10}H_8$ (c). C_{2h} $B_{30}H_8$ contains eight localized in-plane B–H $2c-2e$ σ -bonds along the

Table 1 σ - and π -ELF bonding patterns of D_{6h} B₁₈H₆²⁺, C_{2h} B₃₀H₈, C_{3h} B₃₉H₉²⁻, C_s B₄₂H₁₀, C_{2h} B₄₂H₁₀, and C_{6h} B₇₂H₁₂, with the estimated bifurcation values of ELF _{σ} and ELF _{π} and their averages ELF_{av} indicated

	ELF _{σ}	ELF _{π}	ELF _{av}
D_{6h} B ₁₈ H ₆ ²⁺	 0.55	 0.85	0.70
C_{2h} B ₃₀ H ₈	 0.87	 0.87	0.87
C_{3h} B ₃₉ H ₉ ²⁻	 0.87	 0.74	0.81
C_s B ₄₂ H ₁₀	 0.89	 0.81	0.85
C_{2h} B ₄₂ H ₁₀	 0.88	 0.83	0.86
C_{2h} B ₄₈ H ₁₀	 0.87	 0.73	0.80
C_{6h} B ₇₂ H ₁₂	 0.76	 0.77	0.77

periphery with the occupation numbers of ON=1.92~1.95 |e|, 32 delocalized in-plane 3c-2e σ -bonds (one for each B₃ triangle in the molecular sheet) with ON=1.63~1.97 |e|, four delocalized out-of-plane 5c-2e π -bonds, and five delocalized out-of-plane 6c-2e π -bonds with ON=1.85~1.96 |e|, which together cover the whole molecular sheet. The nine delocalized π -bonds form two aromatic systems around the two hexagonal holes, which share one delocalized 6c-2e π -

bond over the B₆ rhombus between the two hexagonal holes. Such a bonding pattern is unique with respect to that of D_{2h} C₁₈H₁₆ (which contains 19 2c-2e C–C σ -bonds and nine localized C–C 2c-2e π -bonds, see Fig. 3b) and that of D_{2h} C₁₀H₈ (which has 11 2c-2e C–C σ -bonds, four localized 2c-2e π -bonds, and one delocalized 6c-2e π -bond going across the C₂ bridge between the two hexagonal holes, see Fig. 3c) [40–43]. It is important to note that the B₃₀ sheet in

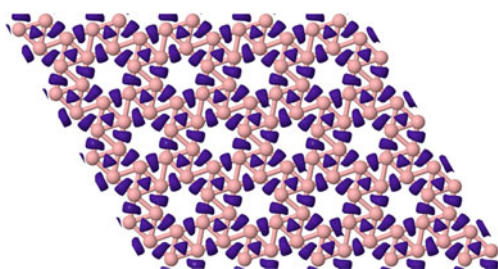


Fig. 4 ELF_{av} of a boron snub sheet with ELF_{av}=0.73

C_{2h} $B_{30}H_8$ possesses only delocalized σ -bonds (32 $3c-2e$ σ -bonds) and π -bonds (four $5c-2e$ π -bonds plus five $6c-2e$ π -bonds) to overcome the electron deficiency of the system, similar to the situation observed in $B_{18}H_6^{2+}$ (**1**) [24]. Such evenly distributed delocalized σ -bonds and π -bonds cover the whole molecular sheet and lead to the formation of islands of both σ - and π -aromaticity in $B_{30}H_8$, similar to the island σ - and π -aromaticities observed in Li_6 [40–43], $B_{18}H_6^{2+}$ [24], and other boron-rich boron hydride clusters [25–27].

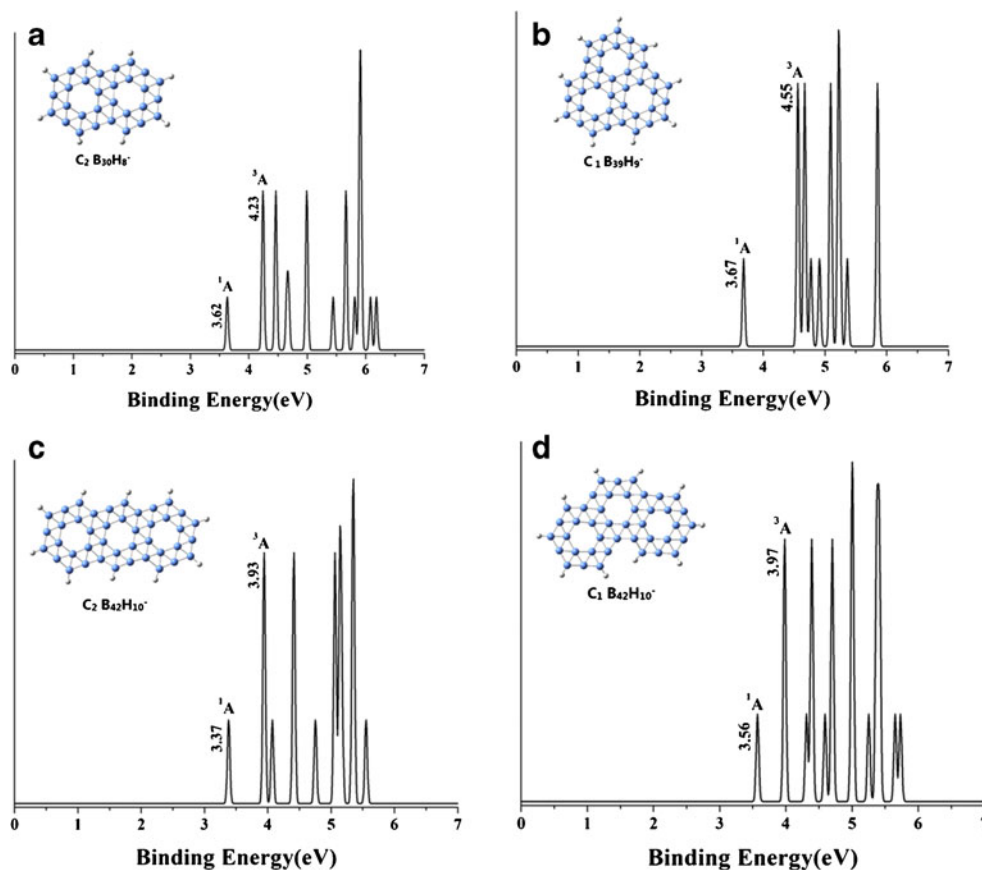
The π -bonding patterns of the monocyclic D_{6h} $B_{18}H_6^{2+}$, dicyclic D_{2h} $B_{30}H_8$, tricyclic C_{3h} $B_{39}H_9^{2-}$, tricyclic C_{2h} $B_{42}H_{10}$, and tricyclic C_s $B_{42}H_{10}$ species are shown schematically in Scheme 2. In this scheme, each circle represents a delocalized π -system (with two neighboring π -systems sharing one delocalized π -bond over the B_6 rhombus region

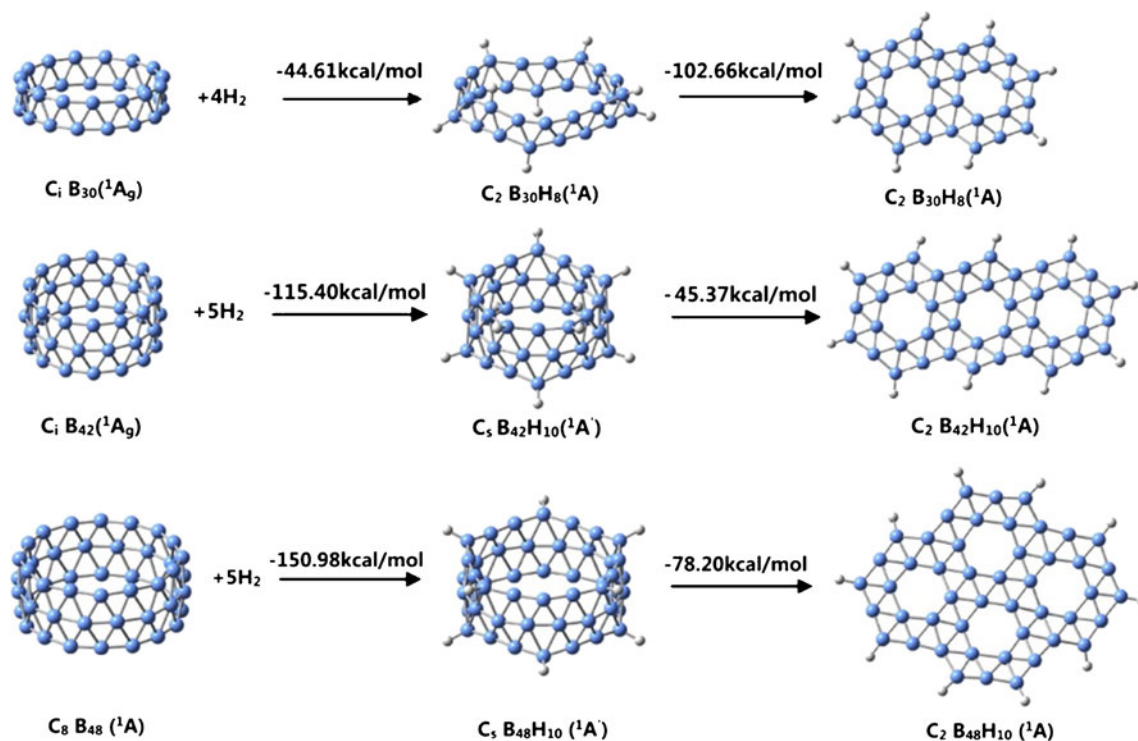
between them). Such bonding patterns appear to be similar to the simplified π -bonding patterns of benzene, naphthalene $C_{10}H_8$, phenalenyl anion $C_{13}H_9^-$, phenanthrene $C_{14}H_{10}$, and anthracene $C_{14}H_{10}$, respectively, further revealing the analogous relationship between PAHBs and their corresponding PAHCs.

ELF analyses

To assess the overall aromaticity of the PAHB clusters explored in this work, we performed detailed ELF analyses of them. ELF_{av} reflects the probability of finding an electron or a pair of pairs in specific basins [44–46]. Based upon extensive benchmark calculations on various organic and inorganic molecules, Santos and coworkers [45] established that aromatic molecules possess average bifurcation values $(ELF_\sigma + ELF_\pi)/2 = ELF_{av} > 0.70$ in the interval (0,1). As shown in Table 1, the perfectly planar PAHB clusters (which are very similar to their fully optimized quasi-planar geometries, as shown in Fig. 1) possess bifurcation values of $ELF_\sigma = 0.55\text{--}0.89$ and $ELF_\pi = 0.73\text{--}0.87$, so that $ELF_{av} = 0.70\text{--}0.87$, indicating that all of the PAHBs explored in this work are aromatic in nature overall based on the ELF criteria, in agreement with the CMO and AdNDP analyses presented above.

Fig. 5 Simulated PES spectra of $C_2 B_{30}H_8^-$ (a), $C_1 B_{39}H_9^-$ (b), $C_2 B_{42}H_{10}^-$ (c), and $C_1 B_{42}H_{10}^-$ (d) obtained at the B3LYP level of theory



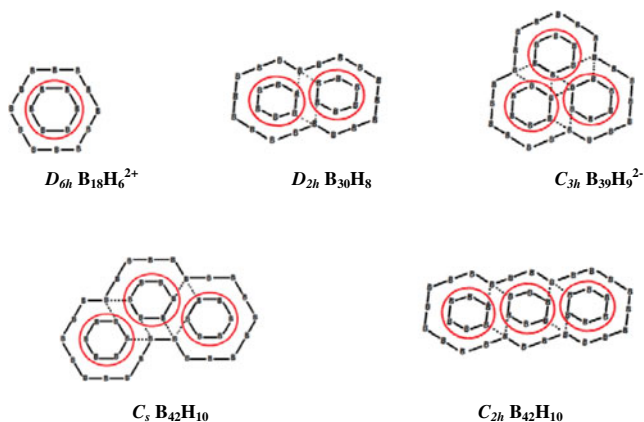


Scheme 1 Hydrogenation energies from the multi-ring tubular B_{30} , B_{42} , and B_{48} to polycyclic snub $B_{30}H_8$, $B_{42}H_{10}$, and $B_{48}H_{10}$

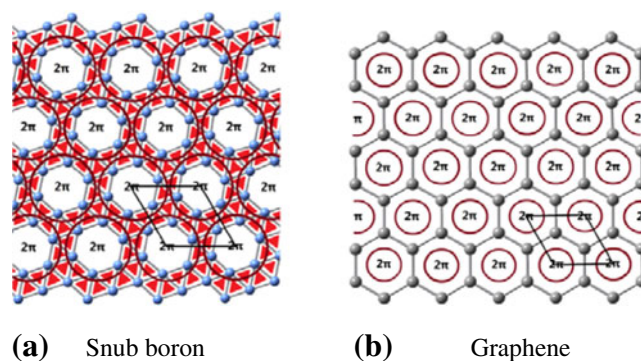
The ELF analyses shown in Table 1 reveal the formation of in-plane 3c-2e σ -bonds in B_3 triangles which share apex atoms with three surrounding hexagonal holes, while each B_3 triangle that shares an edge with one neighboring hexagonal hole possesses a 2c-2e ELF σ -bond along the shared edge. Such 2c-2e σ -bonds with a significant contribution from the third apex atom in the triangle are found to be 3c-2e σ -bonds in AdNDP analyses, as indicated by the AdNDP bonding pattern of $B_{30}H_8$ (**2**) in Fig. 3a, in which each B_3 triangle possesses a 3c-2e σ -bond. A similar situation has been observed in $B_{18}H_6^{2+}$ (**1**) [24]. We also note that the out-of-plane ELF π -bonds of PAHBs shown in Table 1 are highly delocalized in nature, suggesting

that they are similar to the 18c-2e delocalized π -bonds observed in $B_{18}H_6^{2+}$ (**1**) [24]. The central planar B_{18} fragment of $C_{6h} B_{72}H_{12}$ contains typical delocalized σ - and π -bonds of this type (see Table 1), which appear to be similar to the ELF bonding patterns of the snub sheet discussed below.

Detailed ELF analyses have also been performed for the boron snub sheet [38] using the 2D periodic condition. As shown in Fig. 4, with a bifurcation value of 0.73 (which indicates the aromatic nature of the boron snub sheet), the ELF's of the snub sheet contain a 3c-2e σ -bond in each B_3 triangle that shares three apex atoms with three surrounding hexagonal holes, while all of the other B_3 triangles contain 2c-2e σ -bonds with major contributions from the shared edges with neighboring hexagonal holes. As discussed



Scheme 2 π -bonding patterns of $D_{6h} B_{18}H_6^{2+}$, $D_{2h} B_{30}H_8$, $C_{3h} B_{39}H_9^{2-}$, $C_s B_{42}H_{10}$, and $C_{2h} B_{42}H_{10}$



Scheme 3 Comparison of the AdNDP bonding patterns of snub boron (a) and graphene (b)

above, such 2c-2e σ -bonds correspond to 3c-2e σ -bonds in the AdNDP approach. The central concentric planar B_{18} fragment of $C_{6h} B_{72}H_{12}$ exhibits just such a σ -bonding pattern, which is surrounded by six evenly distributed hexagonal holes to simulate the periodic situation in the snub sheet (compare Table 1 and Fig. 4).

Based upon the analyses presented above, we propose the bonding pattern of the boron snub sheet and compare it with the recently reported AdNDP bonding pattern of graphene [57] in Scheme 3 below.

In this scheme, each primitive unit cell with six boron atoms possesses eight delocalized in-plane 3c-2e σ -bonds along the zigzag boron DCs and one out-of-plane 18c-2e π -bond delocalized over the concentric planar B_{18} structural unit (which contains a concentric B_6 inner hexagon ring and a B_{12} outer hexagon ring). The evenly distributed 18c-2e π -bonds are expected to render aromaticity and metallicity to the boron snub sheet. Such a bonding pattern appears to be similar to that of graphene, which possesses three in-plane 2c-2e σ -bonds and one out-of-plane 6c-2e π -bond over a hexagonal hole in each primitive unit cell with two carbon atoms [58]. The atomic ratio of B:C=3:1 between the PAHBs and their PAHC counterparts originates from the fact that PAHBs and PAHCs are hydrogenated fragments of the boron snub sheet and graphene, which contain six boron atoms and two carbon atoms in each unit cell, respectively (as indicated in Scheme 3).

Electron detachment energies

DFT calculations show that $B_{30}H_8$ (**2**), $B_{42}H_{10}$ (**4**), $B_{42}H_{10}$ (**5**), $B_{48}H_{10}$ (**6**), and $B_{72}H_{12}$ (**7**) possess vertical ionization potentials (VIP) of 6.74, 6.15, 6.02, 5.98, and 5.99 eV, respectively. These values support the stability of the concerned PAHB neutrals.

We predicted the vertical detachment energies (VDEs) of the dicyclic $C_2 B_{30}H_8^-$ and $C_1 B_{39}H_9^-$ and tricyclic $C_2 B_{42}H_{10}^-$ and $C_1 B_{42}H_{10}^-$ species at the lowest-lying isomers obtained. As shown in the simulated PES spectra in Fig. 5, the first VDE is 3.62, 3.67, 3.37, and 3.56 eV for $C_2 B_{30}H_8^-$, $C_1 B_{39}H_9^-$, $C_2 B_{42}H_{10}^-$, and $C_1 B_{42}H_{10}^-$, respectively, with energy gaps (ΔE_{gap}) of 0.61, 0.88, 0.56, and 0.41 eV between the first singlet band and the second triplet band. As $C_1 B_{39}H_9^-$ has the biggest energy gap in the series, it may be the easiest monoanion to detect in future PES measurements. The VDE peaks that are close together in binding energy may overlap in PES measurements. The typical symmetric breathing vibrational frequencies at 1037, 1027, and 1049 cm^{-1} calculated for $C_2 B_{30}H_8$ (**2**), $C_1 B_{42}H_{10}$ (**4**), and $C_2 B_{42}H_{10}$ (**5**), respectively, may also be observed in their vibrationally resolved PES spectra to help characterize their PAHB monoanions.

Summary

Based on ab initio calculations, we have proposed a new class of $B_{3n}H_m$ snub PAHB clusters that are inorganic analogs of the corresponding C_nH_m PAHC molecules. These PAHB clusters are all aromatic in nature overall according to the ELF criteria, and exhibit the formation of islands of both σ - and π -aromaticity. More definitive criteria for aromaticity, such as dissected nucleus-independent chemical shifts [58, 59], may be used to further investigate the aromaticity of these polycyclic boron hydride clusters. Based upon the H/Au/BO analogy observed in various boron compounds [17, 18, 25–34], the hydrogen atoms in $B_{3n}H_m$ may be substituted with Au and BO radicals to form snub $B_{3n}Au_m$ and $B_{3n}(BO)_m$, respectively. Results reported in the recent literature [21–27] and the present work for a wide range of boron-rich hydroboron clusters strongly support the analogous relationship between hydroborons and hydrocarbons in dual spaces, and invite attempts to experimentally synthesize and characterize such clusters in the gas phase through partial hydrogenation of the corresponding B_n clusters, in order to open up a new area of boron chemistry. Accumulated experimental and theoretical evidence [2, 17, 18, 21–38] indicates that, similar to carbon, boron may also go planar to form low-dimensional nanostructures with properties analogous to their carbon counterparts.

Acknowledgments This work was jointly supported by the National Science Foundation of China (nos. 20873117 and 21003086) and Shanxi Natural Science Foundation (no. 2010011012-3).

References

1. Cotton FA, Wilkinson G, Murrillo CA, Bochmann M (1999) Advanced inorganic chemistry, 6th edn. Wiley, New York
2. Boustani I (2011) Chem Model 8:1
3. Vincent MA, Schaefer HF (1981) J Am Chem Soc 103:5677
4. Tian SX (2005) J Phys Chem A 109:5471
5. Ricca A, Bauschlicher CW (1997) J Chem Phys 106:2317
6. Curtiss LA, Pople JA (1989) J Chem Phys 91:4809
7. Dias JF, Rasul G, Seidl PR, Surya Prakash GK, Olah GA (2003) J Phys Chem A 107:7981
8. McKee ML, Wang ZX, Schleyer PvR (2000) J Am Chem Soc 122:4781
9. Schleyer PvR, Subramanian G, Dransfeld A (1996) J Am Chem Soc 118:9988
10. Goursot A, Pénigault E, Chermette H, Fripiat JG (1986) Can J Chem 64:1752
11. Jemmis ED, Balakrishnarajan MM, Pancharatna PD (2001) J Am Chem Soc 123:4313
12. Pancharatna PD, Balakrishnarajan MM, Jemmis ED, Hoffmann R (2012) J Am Chem Soc 134:5916
13. Olson JK, Boldyrev AI (2009) Inorg Chem 48:10060
14. Olson JK, Boldyrev AI (2011) Comp Theor Chem 967:1
15. Olson JK, Boldyrev AI (2012) Chem Phys Lett 523:83
16. Olson JK, Boldyrev AI (2011) Chem Phys Lett 517:62

17. Alexandrova AN, Boldyrev AI, Zhai H-J, Wang L-S (2006) *Coord Chem Rev* 250:2811
18. Alexandrova AN, Koyle E, Boldyrev AI (2006) *J Mol Model* 12:569
19. Boyukata M, Ozdogan C, Güvenc ZB (2007) *J Mol Struct (THEOCHEM)* 805:91
20. Yu H-L, Sang RL, Wu YY (2009) *J Phys Chem A* 113:3382
21. Szwacki NG, Weber V, Tymczak CJ, Nanoscale J (2009) *Res Lett* 4:1085
22. Bai H, Li S-D (2011) *J Clust Sci* 22:525
23. Chen Q, Li S-D (2011) *J Clust Sci* 22:513
24. Chen Q, Bai H, Guo J-C, Miao C-Q, Li S-D (2011) *Phys Chem Chem Phys* 13:20620
25. Li D-Z, Lu H-G, Li S-D (2012) *J Mol Model* 18:3161. doi:10.1007/s00894-011-1322-y
26. Li D-Z, Chen Q, Lu H-G, Li S-D (2012) *Phys Chem Chem Phys* (in press; article no. CP-ART-03-2012-040902.R1)
27. Li W-L, Romanescu C, Jian T, Wang L-S (2012) *J Am Chem Soc* 134:13228
28. Sergeeva AP, Zubarev DY, Zhai H-J, Boldyrev AI, Wang L-S (2008) *J Am Chem Soc* 130:7244
29. Huang W, Sergeeva AP, Zhai H-J, Averkiev BB, Wang L-S, Boldyrev AI (2010) *Nat Chem* 2:202
30. Sergeeva AP, Averkiev BB, Zhai H-J, Boldyrev AI, Wang L-S (2011) *J Chem Phys* 134:224304
31. Piazza ZA, Li W-L, Romanescu C, Sergeeva AP, Wang L-S, Boldyrev AI (2012) *J Chem Phys* 136:104310
32. Zhai H-J, Li S-D, Wang L-S (2007) *J Phys Chem A* 111:1030
33. Zhai HJ, Li S-D, Wang L-S (2007) *J Am Chem Soc* 129:9254
34. Li S-D, Zhai H-J, Wang L-S (2008) *J Am Chem Soc* 130:2573
35. Tang H, Ismail-Beigi S (2007) *Phys Rev Lett* 99:115501
36. Yang X, Ding Y, Ni J (2008) *Phys Rev B* 77:0414402
37. Galeev TR, Chen Q, Guo J-C, Bai H, Miao C-Q, Lu H-G, Sergeeva AP, Li S-D, Boldyrev AI (2011) *Phys Chem Chem Phys* 13:11575
38. Zope RR, Baruah T (2010) *Chem Phys Lett* 501:193
39. Novoselov KS, Geim AK, Morozov SV (2004) *Science* 306:666
40. Zubarev DY, Boldyrev AI (2008) *Phys Chem Chem Phys* 10:5207
41. Zubarev DY, Boldyrev AI (2008) *J Org Chem* 73:9251
42. Zubarev DY, Boldyrev AI (2009) *J Phys Chem A* 113:866
43. Galeev TR, Chen Q, Guo J-C, Bai H, Miao C-Q, Lu H-G, Sergeeva AP, Li S-D, Boldyrev AI (2011) *Phys Chem Chem Phys* 13:11575
44. Silvi B, Savin A (1994) *Nature* 371:683
45. Becke A, Edgecombe K (1990) *J Chem Phys* 92:5397
46. Santos JC, Andres J, Aizman A, Fuentealba P (2005) *J Chem Theor Comput* 1:83
47. Beck AD (1993) *J Chem Phys* 98:5648
48. Lee C, Yang W, Parr RG (1988) *Phys Rev B* 37:785
49. Head-Gordon M, Pople JA, Frisch MJ (1988) *Chem Phys Lett* 153:503
50. Saebø S, Almlöf J (1989) *Chem Phys Lett* 154:83
51. Frisch MJ, Head-Gordon M, Pople JA (1990) *Chem Phys Lett* 166:275
52. Frisch MJ, Head-Gordon M, Pople JA (1990) *Chem Phys Lett* 166:281
53. Head-Gordon M, Head-Gordon T (1994) *Chem Phys Lett* 220:122
54. Frisch J, Trucks GW, Schlegel HB, Scuseria GE, Robb MA, Cheeseman JR, Montgomery JA Jr, Vreven T, Kudin KN, Burant JC, Millam JM, Iyengar SS, Tomasi J, Barone V, Mennucci B, Cossi M, Scalmani G, Rega N, Petersson GA, Nakatsuji H, Hada M, Ehara M, Toyota K, Fukuda R, Hasegawa J, Ishida M, Nakajima T, Honda Y, Kitao O, Nakai H, Klene M, Li X, Knox JE, Hratchian HP, Cross JB, Bakken V, Adamo C, Jaramillo J, Gomperts R, Stratmann RE, Yazyev O, Austin AJ, Cammi R, Pomelli C, Ochterski J, Ayala PY, Morokuma K, Voth GA, Salvador P, Dannenberg JJ, Zakrzewski VG, Dapprich S, Daniels AD, Strain MC, Farkas O, Malick DK, Rabuck AD, Raghavachari K, Foresman JB, Ortiz JV, Cui Q, Baboul AG, Clifford S, Cioslowski J, Stefanov BB, Liu G, Liashenko A, Piskorz P, Komaromi I, Martin RL, Fox DJ, Keith T, Al-Laham MA, Peng CY, Nanayakkara A, Challacombe M, Gill PMW, Johnson BG, Chen W, Wong MW, Gonzalezand C, Pople JA (2004) GAUSSIAN03 (revision A.01). Gaussian, Inc., Wallingford
55. Wales DJ, Doye JPK (1979) *J Phys Chem A* 101:5111
56. Tian F-Y, Wang Y-X (2008) *J Chem Phys* 129:024903
57. Popov IA, Bozhenko KV, Boldyrev AI (2012) *Nano Res* 5:117
58. Schleyer PvR, Maerker C, Dransfeld A, Jiao H, Eikema HNJRV (1996) *J Am Chem Soc* 118:6317
59. Fallah-Bagher-Shaidaei H, Wannere CS, Corminboeuf C, Puchta R, Schleyer PvR (2006) *Org Lett* 8:863